Energy Conversion and Management 90 (2015) 446–457

Contents lists available at ScienceDirect

Energy Conversion and Management

journal homepage: www.elsevier.com/locate/enconman

A simulation study on the torrefied biomass gasification

Dhruv Tapasvi [a,*], Rajesh S. Kempegowda [b], Khanh-Quang Tran [a], Øyvind Skreiberg [b], Morten Grønli [a]

[a] *Norwegian University of Science and Technology (NTNU), NO-7491 Trondheim, Norway*
[b] *SINTEF Energy Research, NO-7465 Trondheim, Norway*

ARTICLE INFO

Article history:
Received 1 August 2014
Accepted 16 November 2014
Available online 6 December 2014

Keywords:
Biomass
Gasification
Torrefaction
Energy efficiency
Exergy efficiency

ABSTRACT

Many studies have evaluated biomass behavior in a gasification process. Similar studies with torrefied biomass are needed to evaluate the improvements in biomass properties with torrefaction. This forms the basis of this study. A two-stage biomass gasification model is presented by using Aspen Plus as the simulation and modeling tool. The model included the minimization of the Gibbs free energy of the produced gas to achieve chemical equilibrium in the process, constrained by mass and energy balances for the system. Air and steam were used as the oxidizing agent in the process that uses both untreated and torrefied biomass as feedstocks. Three process parameters, equivalence ratio (ER), Gibbs reactor temperature and steam-to-biomass ratio (SBR), were studied. 27 cases were included in the analysis by operating the system below the carbon deposition boundary with all carbon in gaseous form in the product gas. Product gas composition in the form of hydrogen (H_2), carbon monoxide (CO), carbon dioxide (CO_2), methane (CH_4) and nitrogen (N_2) was analyzed together with cold gas energy and exergy efficiencies for all the cases. Overall, mole fractions of H_2, CO, CO_2 and N_2 were between 0.23–0.40, 0.22–0.42, 0.01–0.09 and 0.14–0.36 for torrefied wood and 0.21–0.40, 0.17–0.34, 0.03–0.09 and 0.15–0.37 for untreated wood, respectively. Similarly, cold gas energy and exergy efficiencies were between 76.1–97.9% and 68.3–85.8% for torrefied wood and 67.9–91.0% and 60.7–79.4% for untreated wood, respectively. Torrefied biomass has higher H_2 and CO contents in the product gas and higher energy and exergy efficiencies than the untreated biomass. Overall efficiencies of an integrated torrefaction–gasification process depend on the mass yields of the torrefaction process. Results from this study were validated using a C–H–O ternary diagram and with results from other similar studies.

© 2014 Elsevier Ltd. All rights reserved.

1. Introduction

Biomass is one of the most important renewable energy sources in the near future. Increased use of biomass can extend the lifetime of our fossil fuel resources. The potential of biomass to help meet the world energy demand has been widely recognized. However, problems such as low bulk density, high moisture content and relatively low calorific value, make biomass an expensive fuel to use and hinder its widespread use. Researchers are looking into solutions to overcome these drawbacks and thus, improve the properties of biomass as a fuel. A lot of research is underway to improve the fuel quality of biomass via torrefaction. Torrefaction is a pretreatment method to upgrade raw biomass to a refined fuel with improved properties such as higher heating value and carbon content and improved grindability. Torrefaction is carried out at 200–300 °C for 30–60 min, in an inert environment at atmospheric pressure. Torrefaction results in the following main improvements in the biomass properties [1–14]:

- considerable reduction in the moisture content;
- increased heating value due to reduction in the O/C ratio, and increased energy density when compressed;
- intrinsic conversion of the hygroscopic behavior of raw biomass into the hydrophobic behavior of torrefied biomass;
- enhanced grindability, which results in less energy consumption during milling.

Because of these improved properties, the value of the torrefied biomass as a fuel is significantly higher than that of the raw biomass.

A promising way to use biomass for production of heat, electricity, and other biofuels is through biomass gasification, in which, through a partial oxidation, the biomass is converted into synthesis gas and condensable compounds. During the gasification the chemical energy of the biomass is converted to the thermal and chemical energy of the synthesis gas [15]. Gasification achieves a

---

[*] Corresponding author. Tel.: +47 93818918; fax: +47 73593580.
E-mail address: dhruv.tapasvi@ntnu.no (D. Tapasvi).

http://dx.doi.org/10.1016/j.enconman.2014.11.027
0196-8904/© 2014 Elsevier Ltd. All rights reserved.

high carbon conversion rate for the formation of syngas [16,17]. Clean synthesis gas (syngas), produced from partial combustion of biomass, can e.g. be burnt in a gas turbine combustion chamber to run a biomass based combined cycle power plant [18]. Biomass can be gasified in various ways by properly controlling the mix of fuel and oxidant within the gasifier. The gasification of coal and biomass began in the 1800s, and by the 1850s, gas light for streets became common. Due to its high efficiency with respect to syngas formation, it is desirable that gasification becomes increasingly applied in the future for biofuels production rather than direct combustion [19].

Many studies have evaluated biomass behavior in a gasification process. Puig-Arnavat et al. [16] reviewed the various gasification models based on thermodynamic equilibrium, kinetics and artificial neural networks. According to Puig-Arnavat et al. [16], thermodynamic equilibrium models have been used widely. For example, Schuster et al. [20] studied the fluidized bed process with main focus on steam gasification; Altafini et al. [21] studied a saw dust gasifier to analyze the operating conditions of an open top stratified downdraft gasifier; Melgar et al. [22] used an equilibrium approach and studied the influence of fuel/air ratio and the moisture content of the biomass on the characteristics of the process and the producer gas composition; Jarungthammachote and Dutta [23,24] used a modified stoichiometric equilibrium approach by accounting for a deviation factor from experiments to three types of gasifiers: a central jet spouted bed, a circular split spouted bed and a spout-fluid bed; Yoshida et al. [25] applied a two-stage equilibrium model for a high temperature gasification process to predict the performance of commercial gasifiers. Similarly, Ghassemi et al. [26], Altafini et al. [21], Bassyouni et al. [27], Ravikiran et al. [28] and Li et al. [29] studied the biomass gasification process by an equilibrium approach based on the minimization of Gibbs free energy. All these authors have shown reasonable agreement between equilibrium predictions and experimental data. Commercial tools such as Aspen Plus are also very useful in predicting the behavior of a biomass gasification process as a sub-model with built-in solids properties. Mansaray et al. [30] used Aspen Plus to simulate a dual-distributor-type fluidised-bed rice husk gasifier. Paviet et al. [31] studied thermo-chemical equilibrium modeling of a biomass gasification process. Based on these studies, it can be concluded that an equilibrium model with Gibbs free energy minimization approach in Aspen Plus is an acknowledged and realistic way of simulating a biomass gasification process.

In a few recent studies, it has been reported that torrefied biomass can significantly affect the efficiency of biomass gasification. Chen et al. [32] employed a process optimization technique, the Taguchi method, for identifying optimum levels for process parameters involved during co-gasification of torrefied biomass and coal in an entrained flow gasifier. In another study, Chen et al. [33] numerically simulated an entrained flow gasifier with oxygen as the gasifying agent and the results indicated that the gasification performance of torrefied bamboo is quite similar to that of coal. Furthermore, Kuo et al. [34] evaluated a two-stage gasification process for raw and torrefied bamboo by using Gibbs minimization approach under isothermal conditions in Aspen Plus simulations. It was reported that the carbon conversion and syngas yield was higher for torrefied materials than the raw biomass, whereas, the trends for cold gas efficiency were opposite. Torrefied biomass produced at 250 °C was found to be the most feasible fuel for gasification when considering all process parameters together. However, this study did not account for tar formation and assumed char as a pure carbon. Except for these few studies, there is a considerable lack of information on the behavior of torrefied biomass under gasification conditions and therefore, better knowledge on the topic is needed. This forms the basis of this present study.

The present work extends the efforts of Kuo et al. [34] to establish a detailed equilibrium model for understanding the effect of torrefaction on the syngas compositions and efficiency of the biomass gasification process. The aim is to study a two-stage gasification process by using Gibbs free energy minimization approach in Aspen Plus with improved accuracy together with a comprehensive thermodynamic analysis. A two-stage process refers to the pyrolysis or decomposition of biomass in the first stage followed by the gasification of the pyrolysis products in the second stage. Accuracy of the model is improved by including tar formation during pyrolysis and its further cracking in the gasification reactor; actual experimental decomposition yields as inputs for both untreated and torrefied biomass; the compositions of the chars produced during pyrolysis, as calculated from the elemental balance; and a C–H–O Ternary diagram for validating the results. The model is integrated with an Excel spreadsheet to study the energy and exergy efficiencies of the process at different operating conditions of the gasifier. Exergy analysis of a process is a supplement to energy analysis and is based on the 2nd law of thermodynamics. It is a very useful tool to assess work potentials of input and output materials and heat streams, and to pinpoint irreversibility losses in a system. Ptasinski [35] studied exergetic efficiency analysis for gasification of biofuels which includes wood, vegetable oil, sludge, and manure. Rao et al. [36] reported results from an investigation of the change in exergy content of the produced gas in gasification for various biomass sources. Pellegreni et al. [37] studied the parametric effect on exergy efficiency by considering the influence of many variables inherent to the model, such as: gasification temperature, moisture content, and air temperature, among others. Abuadala et al. [38] presented an exergy analysis of hydrogen production from gasification. Hosseini et al. [39] also compared energy and exergy for steam fed and air fed gasification systems using sawdust as a fuel. The present study can be regarded as a maiden attempt to carry out a thermodynamic and exergetic efficiency analysis of a gasification process using Gibbs free energy minimization approach in Aspen Plus for comparing untreated and torrefied biomass. Overall efficiencies of an integrated torrefaction–gasification process are also provided by including mass yield in the torrefaction process.

2. Methodology

The Gibbs free energy minimization method for the C–H–O–N atom blend of the biomass fuel and oxidant mixture can be applied for predicting the thermodynamic equilibrium composition of the product gas major components: H_2, CO, CH_4, CO_2, H_2O, N_2 and char [40–43]. A thermodynamic equilibrium model for a biomass gasification system was developed using the Gibbs minimizing approach in the Aspen Plus software as shown in Fig. 1. Material and energy streams data from the Aspen Plus model were used to calculate cold gas energy and exergy efficiencies of the process.

2.1. Aspen Plus model

In Aspen Plus, streams represent mass or energy flows. Mass streams are divided by Aspen Plus into three categories: mixed, solid, and non-conventional (biomass). Mixed streams contain mixtures of components, which can be in gaseous, liquid and solid phases. The solid phase component in this simulation is solid carbon (C). Thermodynamic properties are defined in the Aspen Plus libraries for chemical components. Non-conventional components are defined in Aspen Plus by supplying standard enthalpy of formation and the elementary composition (ultimate and proximate analyses) of the components [44]. Biomass is characterized in this manner in this study.

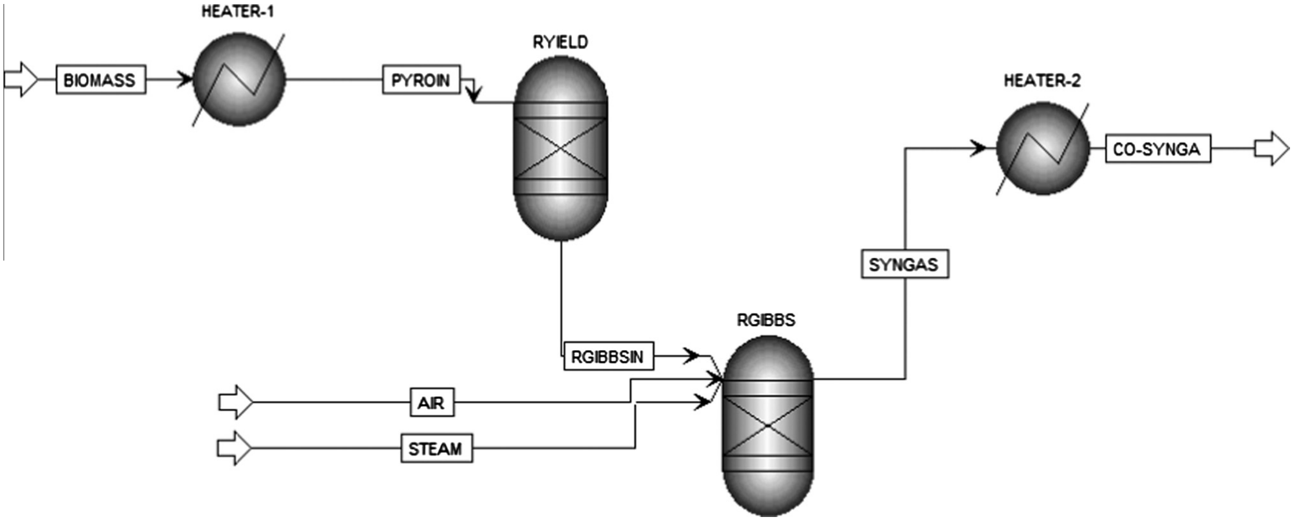

Fig. 1. Gasification process as modeled in Aspen Plus in this study.

2.1.1. Sub-systems

The following sub-systems were included in the modeled gasification process:

(a) Aspen Plus heat exchanger, HEATER, was used to simulate pre-heating of the biomass to a pyrolyzer temperature of 500 °C.
(b) Aspen Plus yield reactor, RYIELD, was used to simulate decomposition of biomass into individual elemental components at 500 °C. This is done by specifying actual experimental yield values for volatiles and char, as available in literature [45].
(c) Aspen Plus Gibbs reactor, RGIBBS, was used for partial combustion of volatiles and char with the addition of air and steam. RGIBBS models chemical equilibrium by minimizing Gibbs free energy, subject to element balance constraints. This model is useful when temperature and pressure are known and reaction stoichiometry is unknown. Both isothermal and adiabatic modeling options are available in the setup of the RGIBBS. Temperature or the heat duty for the RGIBBS unit needs to be specified for these options, respectively. A number of approximations need to be applied for estimating the heat duty for an actual reactor. Therefore, in order to simulate more closely the real conditions in a gasifier, an isothermal approach was used in this study.
(d) Aspen Plus heat exchanger, HEATER, was used to simulate cooling of syngas from RGIBBS temperature to ambient temperature.

2.1.2. Model input data

Based on a recent literature review, only one journal article by Wannapeera et al. [45] listed an experimentally obtained pyrolysis gas composition for both untreated and torrefied biomass. Therefore, the feedstocks used by Wannapeera et al. [45] have been used for this present simulation study. Proximate and ultimate analysis data for the feedstocks and the pyrolysis product yields at 500 °C are listed in Tables 1 and 2, respectively. Torrefied biomass was produced at 250 °C with 30 min of residence time. Starting from the ultimate analysis of biomass and mass fractions of all elements, the biomass formula $C_{a1}H_{a2}O_{a3}N_{a4}$ was calculated by assuming that a_1 is equal to 1.0 by the following Eqs. (1)–(3) [42]:

$$a_2 = \frac{\text{mass fraction(H)} \times \text{Molecular weight(C)}}{\text{mass fraction(C)} \times \text{Molecular weight(H)}} \tag{1}$$

$$a_3 = \frac{\text{mass fraction(O)} \times \text{Molecular weight(C)}}{\text{mass fraction(C)} \times \text{Molecular weight(O)}} \tag{2}$$

$$a_4 = \frac{\text{mass fraction(N)} \times \text{Molecular weight(C)}}{\text{mass fraction(C)} \times \text{Molecular weight(N)}} \tag{3}$$

Based on Eqs. (1)–(3), formulas for the feedstocks are calculated: Biomass $CH_{1.77}O_{0.63}N_{0.012}$; torrefied biomass $CH_{1.45}O_{0.57}N_{0.011}$.

2.1.3. Key process variables

It has been reported that the optimal gasification operation involves operating a gasifier at or below the carbon boundary point, that means that all carbon is present in the gaseous phase as carbon monoxide, carbon dioxide or methane [46]. This theory has been applied for this study as well and all the 27 tested cases have carbon in its gaseous form. This is the basis for selecting the ranges for the three process variables listed in Table 3. ER is defined as the amount of air added relative to the stoichiometric air requirement for combustion and SBR is defined as the ratio of steam to biomass molar flow rates.

Steam is added to the system to improve the hydrogen production and thus increase the syngas quality [42]. Each of the 27 cases will be referred to using these three process variables, as SBR–GB–ER, in this study.

2.1.4. Assumptions made for Aspen Plus simulation and efficiency calculations

(a) All gases behave ideally.
(b) The process occurs at steady state, and residence time was not considered.
(c) Biomass mass flow rate was calculated for a 10 MW fuel input plant.
(d) Air was introduced to RGIBBS at ambient temperature and pressure.
(e) Saturated steam was introduced to RGIBBS at 179.9 °C and 10 bar pressure.
(f) Atmospheric pressure was assumed in all equipment.
(g) The process was assumed to be autothermal and the pressure drop and heat losses from the equipment and pipelines were not included.
(h) Ambient conditions data for each stream was collected from Aspen Plus in order to have consistent values for the reference conditions in the physical exergy calculations.

Table 1
Proximate and ultimate analyses of the samples [45].

Sample	Proximate analysis[a]			Ultimate analysis[a]				HHV[b]
	VM	fC	Ash	C	H	O	N	
Leucaena	86.1	13.1	0.8	50.1	7.4	41.8	0.7	20.3
Torrefied Leucaena	82.2	16.9	0.9	53.0	6.4	39.9	0.7	21.2

[a] % (m/m), dry basis.
[b] MJ/kg, dry basis.

Table 2
Pyrolysis products yield as input to RYIELD [45].

Sample	Pyrolysis product molar yield at 500 °C					
	Char	H_2O	Tar	CO	CH_4	CO_2
Leucaena	0.20	0.20	0.40	0.019	0.001	0.18
Torrefied Leucaena	0.29	0.16	0.34	0.029	0.001	0.18

Table 3
Tested ranges for process variables that resulted in 27 cases.

Process variable	Low	Mid	High
SBR	0.2	0.3	0.4
Gibbs (GB) Temperature (°C)	900	1000	1100
ER	0.1	0.2	0.3

(i) No physical exergy is associated with biomass as these were assumed to be at ambient temperature and pressure.
(j) Minor products such as sulfur species (e.g. S, COS and H_2S) and nitrogen species except N_2 were not included in the chemical exergy of the streams as these are present, relatively speaking, in very negligible amounts.
(k) Kinetic and potential exergies were ignored in the analysis.
(l) No work exergy was included in the exergy analysis.
(m) All biomass feedstocks were completely dry.
(n) Tar was considered as a mixture of 70% secondary (phenol), 14% tertiary-alkyl (xylene) and 16% tertiary-PNA (benzene) components on mass basis [47,48]. Based on the previous studies on tar cracking, it was assumed that tertiary-PNA component is not cracked at all and tertiary-alkyl component is 80% cracked at the temperatures conditions used in this study [48]. In addition to this, untreated biomass is assumed to have 10% aqueous phase acid (acetic acid), which remains un-reacted in RGIBBS [49]. For the torrefied biomass, these acids were assumed to be removed during torrefaction. Char composition of pyrolyzed biomass (from both untreated and torrefied biomass) was calculated from the elemental carbon, hydrogen and oxygen balance based on the assumed tar composition.

2.2. Methods for cold gas energy and exergy efficiencies

The cold gas efficiency of gasification in an allothermal plant is defined in Eq. (4) [40]:

$$\eta_{\text{energy,coldgas}} = \frac{\text{LHV}_{\text{coldgas}}}{\text{LHV}_{\text{biomass}} + Q_{\text{air}} + Q_{\text{steam}}} \tag{4}$$

where $\text{LHV}_{\text{coldgas}}$ is the heating value of the outgoing (product) heat stream; $\text{LHV}_{\text{biomass}}$, Q_{steam} and Q_{air} are the heating value and heat contents of incoming biomass, steam and air streams, respectively. Exergy is the maximum work that can be produced when a heat or material stream is brought to equilibrium relative to a reference environment, which consists of reference components and which is characterized by absence of pressure and temperature gradients. Exergy associated with a material stream is expressed as the sum of its physical and chemical exergies.

The total exergy of a material stream is given by Eq. (5) [40,50]:

$$E = N(\varepsilon_{\text{ph}} + \varepsilon_{\text{ch}}) \tag{5}$$

where N is the flow rate. The molar physical exergy of a material stream is expressed in relation to the reference environmental conditions as shown in Eq. (6) [40,50]:

$$\varepsilon_{\text{ph}} = (h - h_0) - T_0(s - s_0) \tag{6}$$

Mole flows, mole fractions, enthalpy and entropy of each material stream were taken from the Aspen Plus flowsheet results. The standard environmental conditions of Aspen Plus ($T_0 = 25$ °C, $p_0 = 1.013$ bar) were adopted as reference conditions in the study. The molar chemical exergy of a gaseous material mixture is given by Eq. (7) [40,50]:

$$\varepsilon_{\text{ch,gas}} = \sum_i x_i \varepsilon_{0,i} + RT_0 \sum_i x_i \ln x_i \tag{7}$$

where x_i is the mole fraction and $\varepsilon_{0,i}$ is the standard molar chemical exergy of each component i, in J mol^{-1}. The latter is available in literature for the reference atmospheric composition [51].

The chemical exergy of solid fuels (biomass and torrefied product) was calculated with the help of the ratio of the chemical exergy to the lower heating value of the dry matter as shown in Eq. (8) [52]. This ratio is a function of the elemental contents of the solid fuel.

$$\varphi_{\text{dry}} = \frac{\varepsilon_{\text{dm}}}{h_{\text{LHV}_{\text{dm}}}} \tag{8}$$

For dry solid fuels with a certain content of oxygen, the ratio of chemical exergy to lower heating value for the dry matter is expressed in Eq. (9) [52]:

$$\varphi_{\text{dry}} = \frac{1.0438 + 0.1882\frac{h}{c} - 0.2509\frac{o}{c}\left(1 + 0.7256\frac{h}{c}\right) + 0.0383\frac{n}{c}}{1 - 0.3035\frac{o}{c}} \tag{9}$$

Here, h/c is the ratio of hydrogen mass to carbon mass in the fuel, and n/c and o/c correspondingly for nitrogen and oxygen. This expression is valid for o/c from 0.667 to 2.67, and is expected to be accurate within ±1%. Using Eqs. (5)–(9), exergy was calculated for all material streams in the flow sheet. The exergetic efficiency of gasification in an autothermal plant is defined in Eq. (10) [40]:

$$\eta_{\text{exergy,coldgas}} = \frac{E_{\text{coldgas}}}{E_{\text{biomass}} + E_{\text{air}} + E_{\text{steam}}} \tag{10}$$

where E_{coldgas} is the outgoing (product) exergy stream, and E_{biomass}, E_{steam} and E_{air} are the incoming biomass (or the torrefied biomass), steam and air exergies.

Table 4 lists the standard chemical exergy and standard lower heating values of the gases that form syngas [53–55].

Table 4
Standard chemical exergy and LHV values of gases.

Reference data	CO (g)	CO_2 (g)	H_2 (g)	N_2 (g)	H_2O (g)
Standard chemical exergy (MJ/kmol)	275.1	19.87	236.1	0.72	9.5
Standard LHV (MJ/kg)	10.112	0	119.96	0	0

3. Results and discussions

3.1. Syngas compositions

Mole fractions of hydrogen (H_2), carbon monoxide (CO), carbon dioxide (CO_2), and nitrogen (N_2) in the syngas generated from all 27 cases are shown in Figs. 2–5. For improved understanding for the readers, the effect of the three process variables SBR, GB Temperature and ER on these mole fractions is shown separately in Figs. 6–8, where two of these variables are fixed and one is varied. In previous studies in the literature, methane production decreases sharply at temperatures above 500 °C [22,56]. Similar trends were observed in this study and negligible amounts of methane is produced (mole fractions close to 1×10^{-5}) since the temperatures tested are close to 1000 °C. Therefore, the methane content is not reported in these results. Table 5 lists the trends for the syngas content based on increase in any one of the process variables.

These trends are explained in terms of common gasification reactions as listed below (Eqs. (11)–(18)) [57]. Heat of reactions are provided in the brackets for these reactions, with minus sign for exothermic and plus sign for endothermic reactions:

Char partial combustion reaction

$$C + 0.5O_2 = CO \quad (-111\ \mathrm{MJ/kmol}) \tag{11}$$

Boudouard reaction

$$C + CO_2 \Longleftrightarrow 2CO \quad (+172\ \mathrm{MJ/kmol}) \tag{12}$$

Water gas reaction

$$C + H_2O \Longleftrightarrow CO + H_2 \quad (+131\ \mathrm{MJ/kmol}) \tag{13}$$

Methanation reaction

$$C + 2H_2 \Longleftrightarrow CH_4 \quad (-75\ \mathrm{MJ/kmol}) \tag{14}$$

CO partial combustion reaction

$$CO + 0.5O_2 = CO_2 \quad (-283\ \mathrm{MJ/kmol}) \tag{15}$$

H_2 partial combustion reaction

$$H_2 + 0.5O_2 = H_2O \quad (-242\ \mathrm{MJ/kmol}) \tag{16}$$

CO shift reaction

$$CO + H_2O \Longleftrightarrow CO_2 + H_2 \quad (-41\ \mathrm{MJ/kmol}) \tag{17}$$

Steam-methane reforming reaction

$$CH_4 + H_2O \Longleftrightarrow CO + 3H_2 \quad (+206\ \mathrm{MJ/kmol}) \tag{18}$$

As reactions (11)–(14) have carbon in solid state, applicability of these reactions is up to the carbon boundary point. These reactions can explain the differences in the gasification behaviors of torrefied wood and untreated wood based on their carbon contents. Since approximately 70–80% devolatilization of biomass has already occurred in RYIELD (experimental values from Wannapeera et al. [45]), the main reactions happening in RGIBBS are the gas phase reactions (15)–(18).

3.1.1. Effect of increase in SBR

The main reaction by an increase in SBR is the CO shift reaction where CO reacts with steam (H_2O) to form CO_2 and H_2. This results in decrease of CO and increase of CO_2 and H_2 production.

3.1.2. Effect of increase in GB Temperature

Increase in Gibbs reactor temperature also involves the CO shift reaction but in the opposite direction. As the CO shift reaction is exothermic (heat of reaction = −41 MJ/kmol), increase in temperature results in the formation of CO and H_2O from CO_2 and H_2.

3.1.3. Effect of increase in ER

Increase in ER results in CO and H_2 partial combustion where these two gases react individually with oxygen to form CO_2 and H_2O, respectively. Also, air increases the nitrogen content of syngas. These two reactions result in increased CO_2 and H_2O production and decreased CO and H_2 contents.

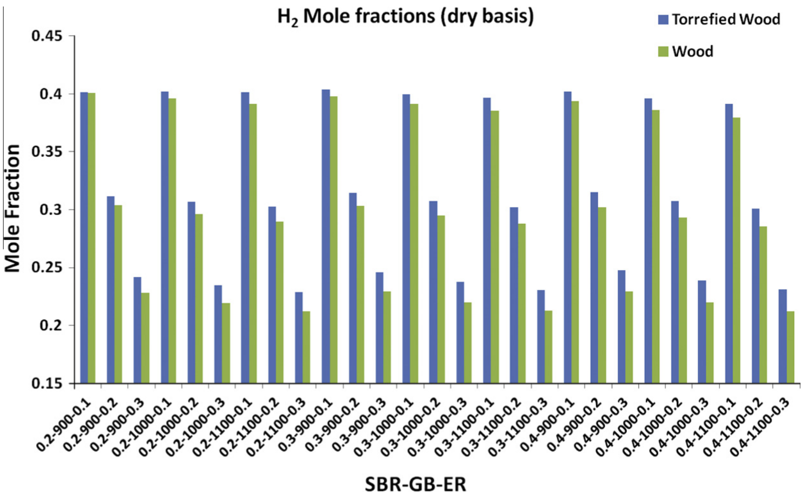

Fig. 2. Hydrogen mole fractions on dry basis for all cases.

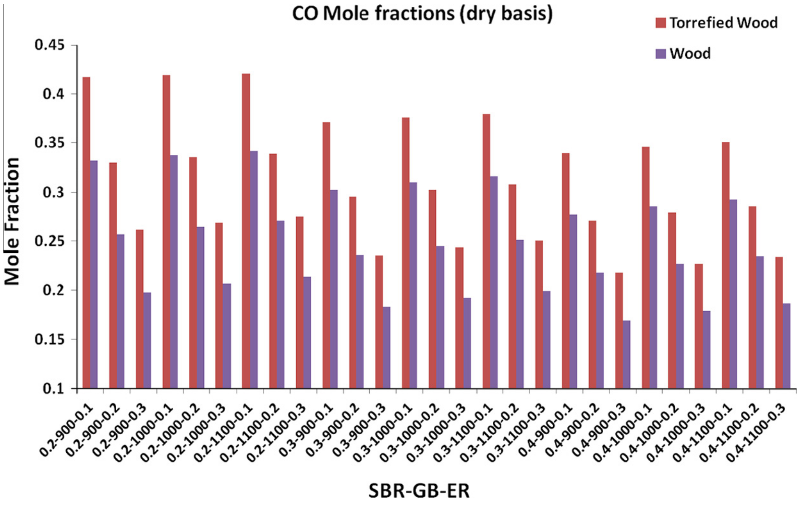

Fig. 3. Carbon monoxide mole fractions on dry basis for all cases.

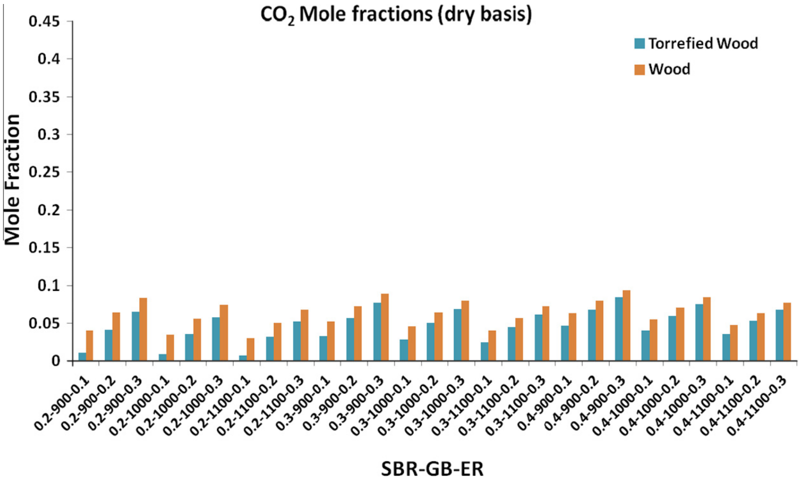

Fig. 4. Carbon dioxide mole fractions on dry basis for all cases.

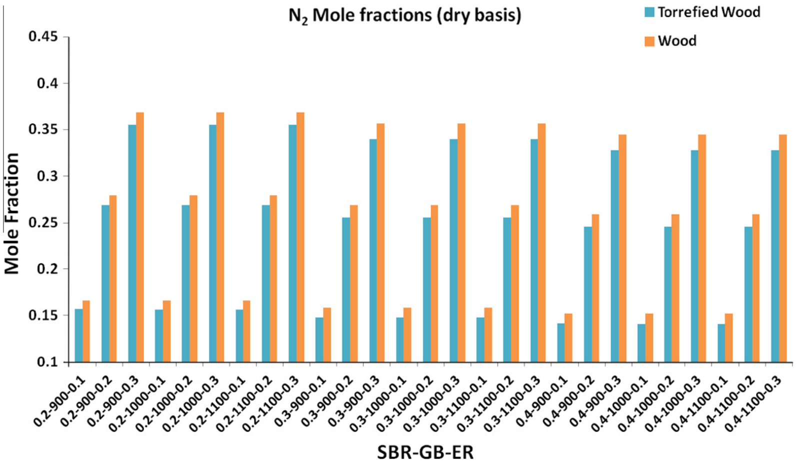

Fig. 5. Nitrogen mole fractions on dry basis for all cases.

3.1.4. Differences between torrefied wood and untreated wood

Torrefied wood results in higher CO and H_2 production in comparison to untreated wood due to higher carbon content. Char partial combustion, Boudouard and water–gas reactions occur with carbon in solid state to form CO and H_2.

3.2. Cold gas energy and exergy efficiencies

Cold gas energy and exergy efficiencies of all the 27 cases are shown in Figs. 9 and 10, respectively. The general trends are listed in Table 6. It can be seen that both energy and exergy efficiencies

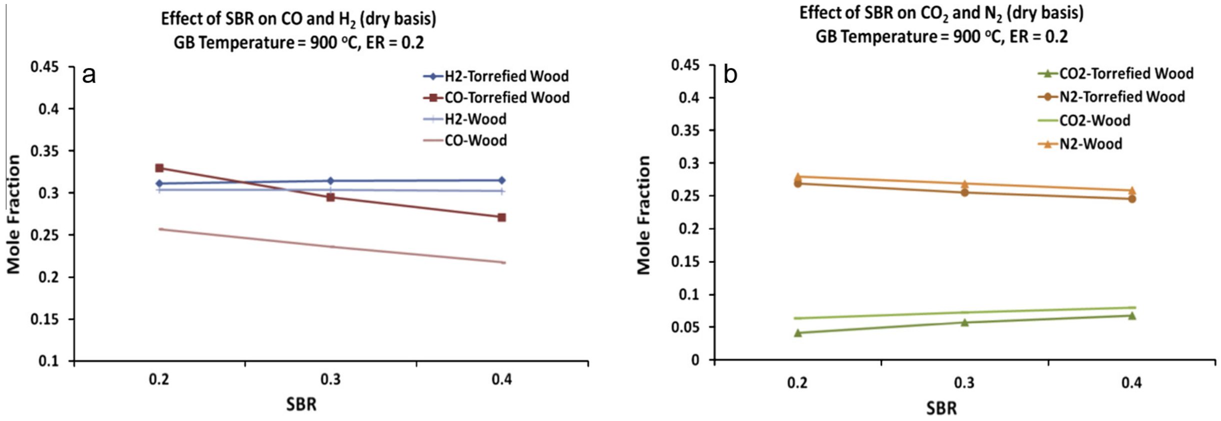

Fig. 6. Effect of SBR on the carbon monoxide and hydrogen (a) and carbon dioxide and nitrogen (b) mole fractions.

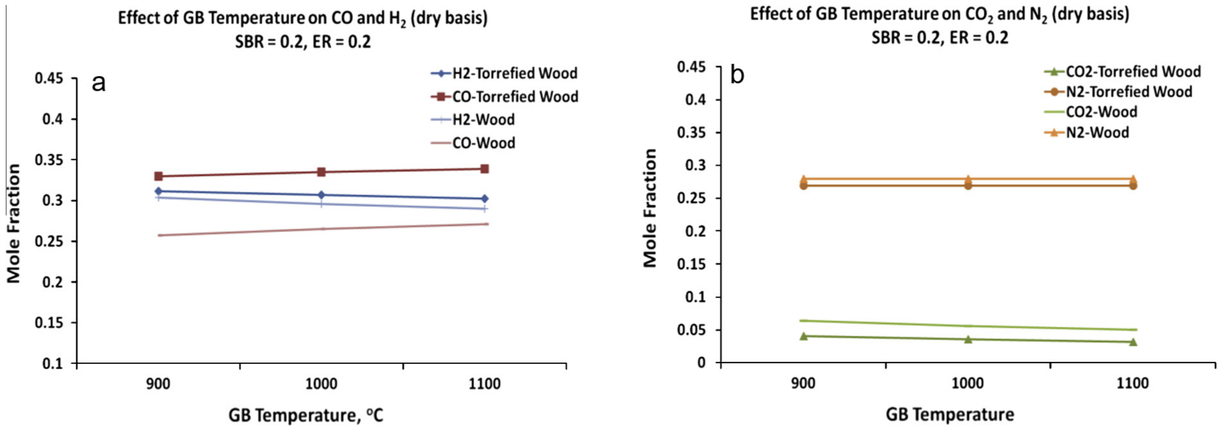

Fig. 7. Effect of GB Temperature on the carbon monoxide and hydrogen (a); carbon dioxide and nitrogen (b) mole fractions.

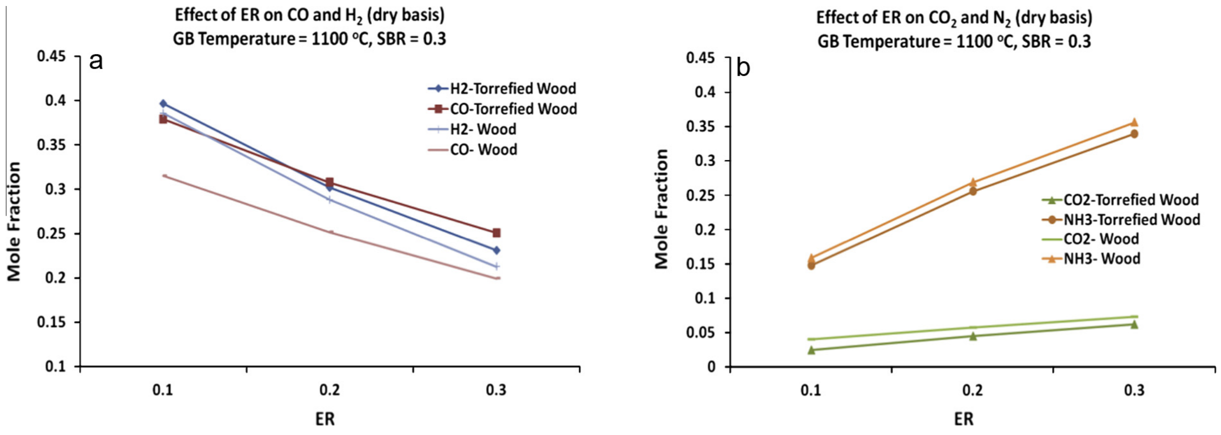

Fig. 8. Effect of ER on the carbon monoxide and hydrogen (a); carbon dioxide and nitrogen (b) mole fractions.

Table 5
Syngas composition trends with changes in SBR, GB Temperature and ER.

Mole fractions	Increase in SBR	Increase in GB Temperature	Increase in ER	Torrefied wood (TW) vs. Wood (W)
H_2	Slightly increases	Slightly decreases	Decreases	TW > W
CO	Decreases	Slightly increases	Decreases	TW > W
CO_2	Slightly increases	Slightly decreases	Increases	W > TW
N_2	Slightly decreases	Negligible effect	Increases	W > TW

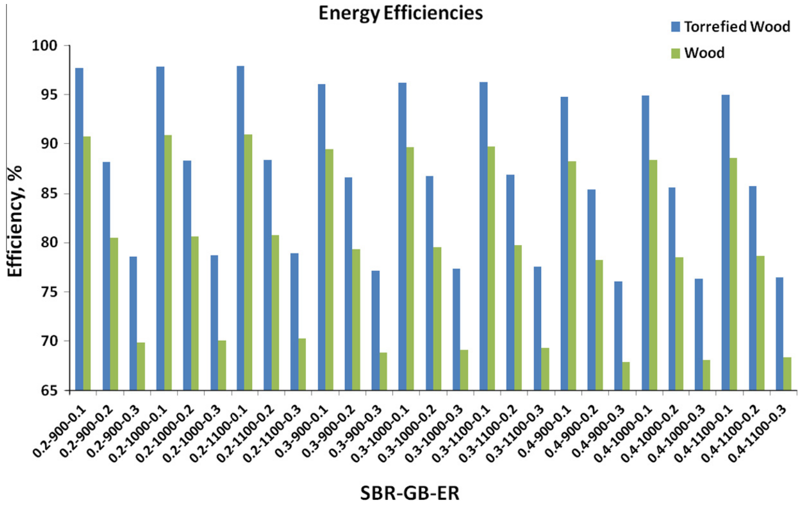

Fig. 9. Cold gas energy efficiencies in percent for all 27 cases.

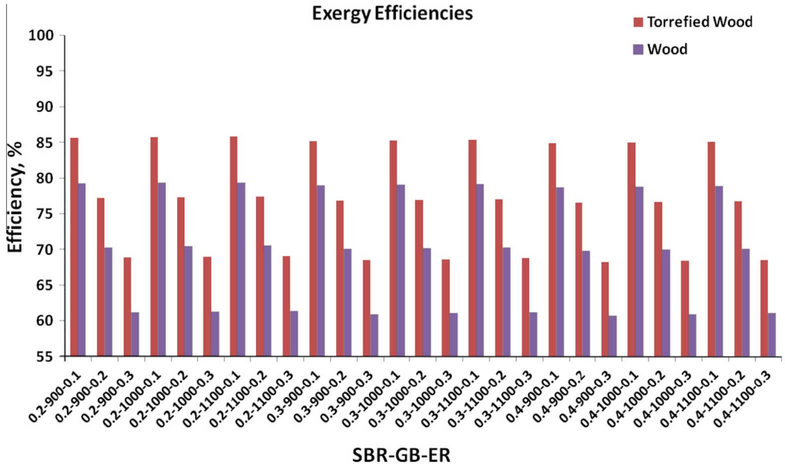

Fig. 10. Exergy efficiencies in percent for all 27 cases.

decrease with increase in SBR, GB Temperature and ER, with ER having the most pronounced effect. Fig. 11(a), (b) and (c) shows the effect of process variables on these efficiencies by varying one of these variables and keeping the other two constant. From Figs. 9–11 it can also be seen that the torrefied wood has higher energy and exergy efficiencies than untreated wood for all cases. Table 7 lists the maximum and minimum values of the energy and exergy efficiencies for all cases.

3.2.1. Effect of increase in SBR

Increase in SBR results in increased CO_2 and H_2 production and decreased CO production. As can be seen from Table 4, standard chemical exergy and standard lower heating values (LHV) for H_2 is lower than for CO and the values for CO_2 are negligible. This results in lower LHV and chemical exergy of the cold syngas and thus, lower energy and exergy efficiencies with increasing SBR.

3.2.2. Effect of increase in GB Temperature

With increasing GB Temperature, CO and H_2O production increases and that of CO_2 and H_2 decreases. Since H_2O and CO_2 have zero LHVs and negligible standard chemical exergies, the increase in CO is compensated by the decrease in H_2. End result is slightly lower (almost constant) energy and exergy efficiencies with the increase in the Gibbs reactor temperature.

3.2.3. Effect of increase in ER

Increase in ER results in increased CO_2, H_2O and N_2 production and decreased CO and H_2 contents. As CO_2, H_2O and N_2 have very low exergy and zero LHV values, reduction in CO and H_2 results in lower syngas chemical exergy and LHV. This results in lower energy and exergy efficiencies with increase in ER.

3.2.4. Differences between torrefied wood and untreated wood

Higher energy and exergy efficiencies for torrefied wood in comparison to untreated wood is mainly attributed to its higher carbon content, which results in higher H_2 and CO contents and thus higher syngas LHV and chemical exergy.

3.2.5. Integrated torrefaction–gasification process

Overall efficiencies of an integrated torrefaction–gasification process can be calculated by including the mass flow rates of the untreated biomass needed for the production of torrefied biomass. Higher mass yields in the torrefaction process will result in improved overall efficiencies of the integrated process. For the current study, torrefied Leucaena has 5.78% higher carbon content than untreated Leucaena in the ultimate analysis with torrefaction at 250 °C for 30 min. For similar torrefaction temperature and residence time and with 8.7% increase in carbon content, mass yields reported in the literature are around 88–90% [2,58]. By using 88%

Table 6
Cold gas energy and exergy efficiency trends.

Efficiency	Increase in SBR	Increase in GB Temperature	Increase in ER	Torrefied wood (TW) vs. Wood (W)
Energy efficiency	Slightly decreases	Slightly decreases	Decreases	TW > W
Exergy efficiency	Slightly decreases	Slightly decreases	Decreases	TW > W

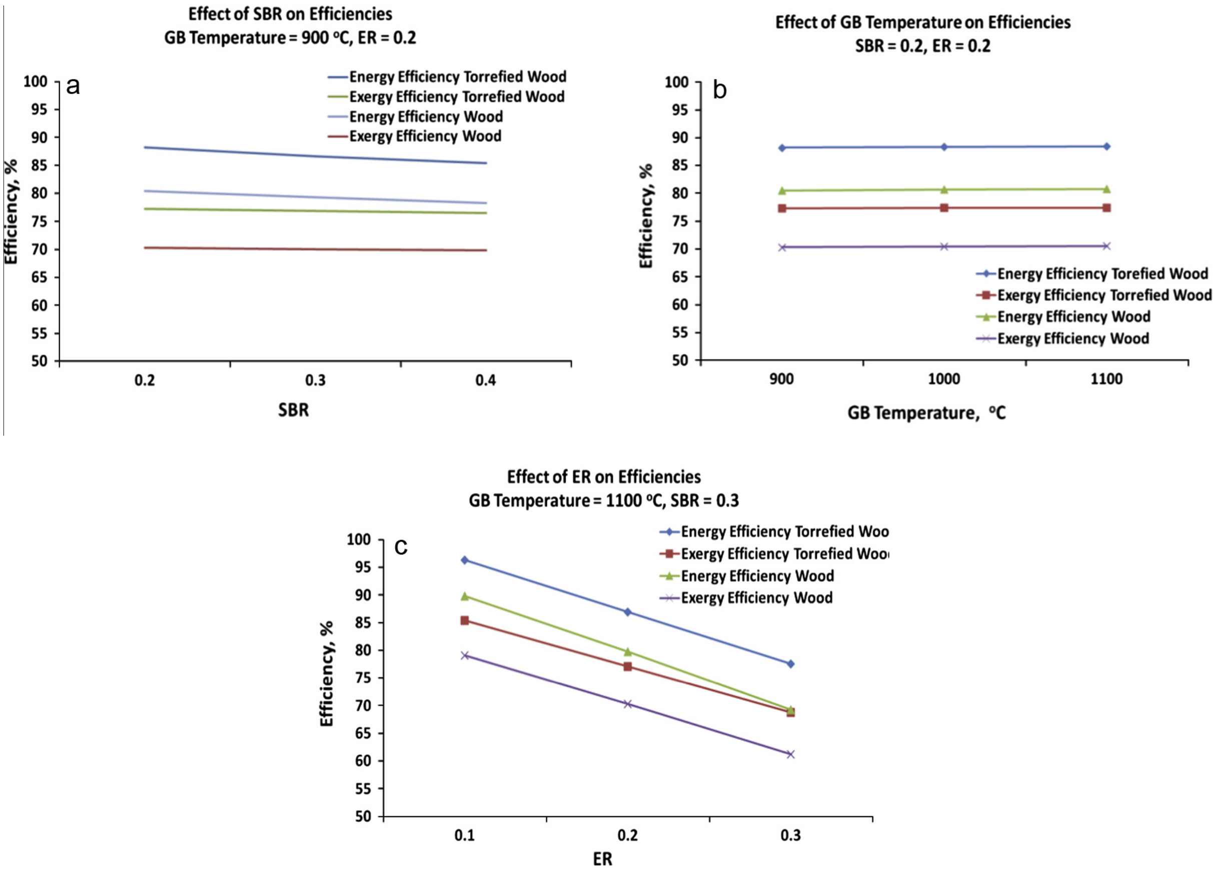

Fig. 11. Effect of SBR (a), GB Temperature (b) and ER (c) on efficiencies.

Table 7
Maximum and minimum efficiencies.

Efficiency		% (TW)	% (W)	SBR	GB Temperature (°C)	ER
Energy efficiency	Maximum	97.9	91.0	0.2	1100	0.1
	Minimum	76.1	67.9	0.4	900	0.3
Exergy efficiency	Maximum	85.8	79.4	0.2	1100	0.1
	Minimum	68.3	60.7	0.4	900	0.3

as torrefaction mass yield for the current study, energy and exergy efficiencies for the integrated process were calculated for a few selected cases. For all of these cases, efficiencies for the integrated process were found to be higher than the stand alone process with untreated biomass as feedstock, as shown in Fig. 12. Effects of the varied process parameters (SBR, GB Temperature and ER) on the efficiencies is similar to the stand alone biomass gasification process.

Efficiencies for the torrefaction process can also be calculated by dividing LHV or the exergy values of torrefied biomass with the corresponding values for untreated biomass. With 88% mass yield and required torrefied biomass production for a 10 MW fuel input plant, energy and exergy efficiencies for the torrefaction process are 93.3% and 92.6%, respectively. Mass yields in a torrefaction process are highly dependent on the choice of the reactor, heat and mass transfer profiles, process control and the production scale. Reactors used at a laboratory scale may not be a good simulation for pilot or industry scale reactors. Therefore, overall efficiencies of an integrated torrefaction–gasification industrial process should be evaluated for a specific reactor type.

3.3. Comparisons of results with other similar studies

For both torrefied and untreated woods, the ranges for the mole fractions of H_2, CO, CO_2 and N_2 in the 27 cases are listed in Table 8.

Based on a literature review, it was found that there is a considerable lack of data for two-stage biomass gasification. The simulation work performed by Paviet et al. [56] is the only one that can be compared to the present work and the results from that study are listed in Table 9. Even though Paviet et al. [56] utilized different

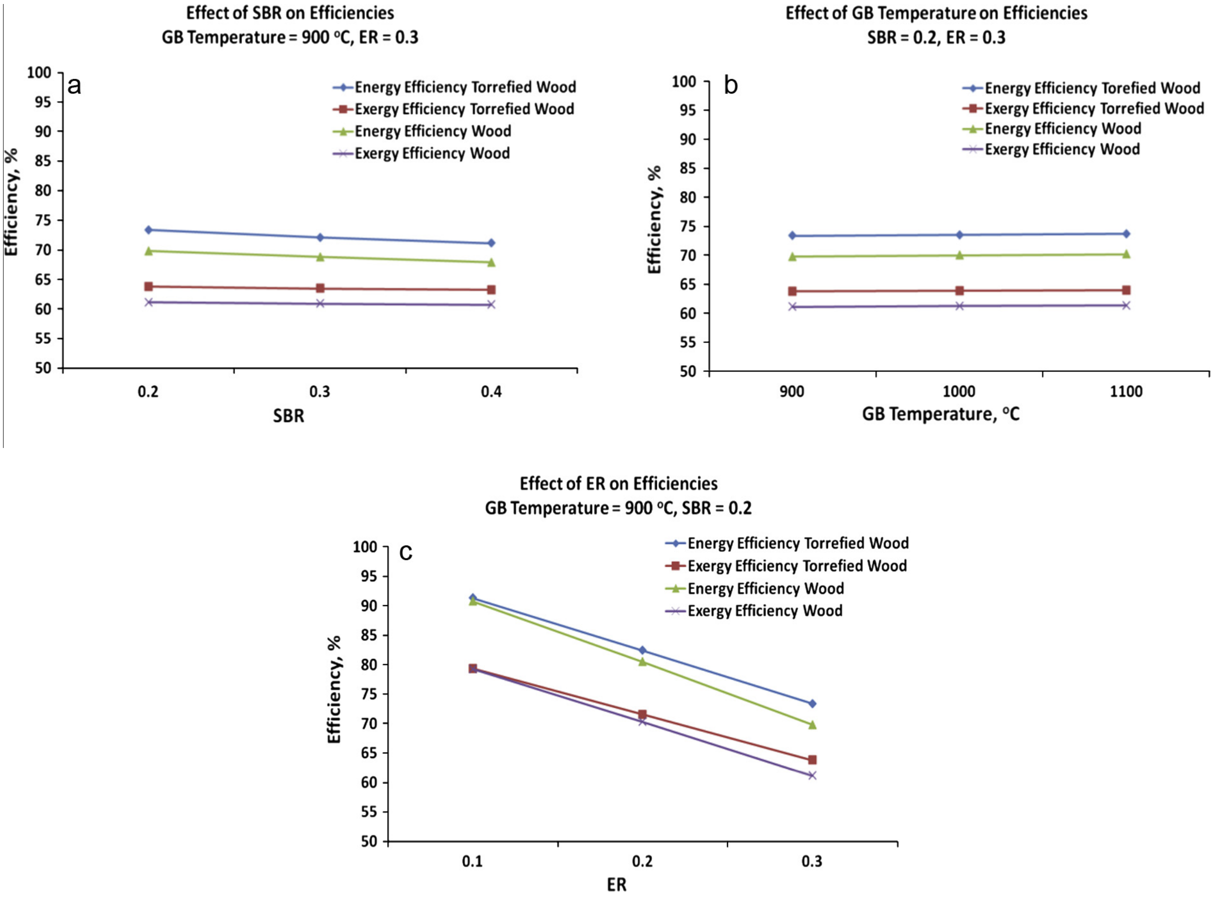

Fig. 12. Effect of SBR (a), GB Temperature (b) and ER (c) on the efficiencies of an integrated torrefaction–gasification process (88% mass yield for torrefaction).

Table 8
Product gas composition.

Syngas components		Mole fraction (TW)	Mole fraction (W)	SBR	GB Temperature (°C)	ER
H_2	Maximum	0.40	0.40	0.3	900	0.1
	Minimum	0.23	0.21	0.3	1100	0.3
CO	Maximum	0.42	0.34	0.2	1100	0.1
	Minimum	0.22	0.17	0.4	900	0.3
CO_2	Maximum	0.09	0.09	0.4	900	0.3
	Minimum	0.01	0.03	0.2	1100	0.1
N_2	Maximum	0.36	0.37	0.2	900	0.3
	Minimum	0.14	0.15	0.4	1100	0.1

operating conditions in the simulation, the two-stage gasification is similar to this present study.

By comparing results from Tables 8 and 9, it can be seen that the syngas contents are quite similar in both studies. The end results for H_2, CO, CO_2 and N_2 are very comparable to both simulation and experimental results from Paviet et al. [56], depending upon the selection of process conditions from the present study. Recently, a few studies have utilized the concept of C–H–O Ternary diagram to show the biomass gasification process with respect to the carbon deposition boundaries [46,59]. Fig. 13 shows the C–H–O ternary diagram for the present study for one case (SBR–GB–ER = 0.3–900–0.2) using the calculation methods mentioned in the literatures [46,59].

In Fig. 13, point A represents untreated biomass, point B represents the syngas produced from RGIBBS. Corresponding points for the torrefied biomass are A′ and B′ respectively. As can be seen,

Table 9
Results from Paviet et al. [56] (dry basis).

Results from Paviet et al.	H_2	CO	CH_4	CO_2	N_2
Simulation results (H: 18.2%, *T*: 1300 K, Ra: 2.53, Rh: 0.40)	0.34	0.26	0.00	0.10	0.30
Experimental results from two-stage gasifier DTU	0.30	0.20	0.01	0.15	0.34

H = Moisture content of fuel; Ra = Air/fuel mass flow ratio; Rh = Steam/fuel mass flow ratio.

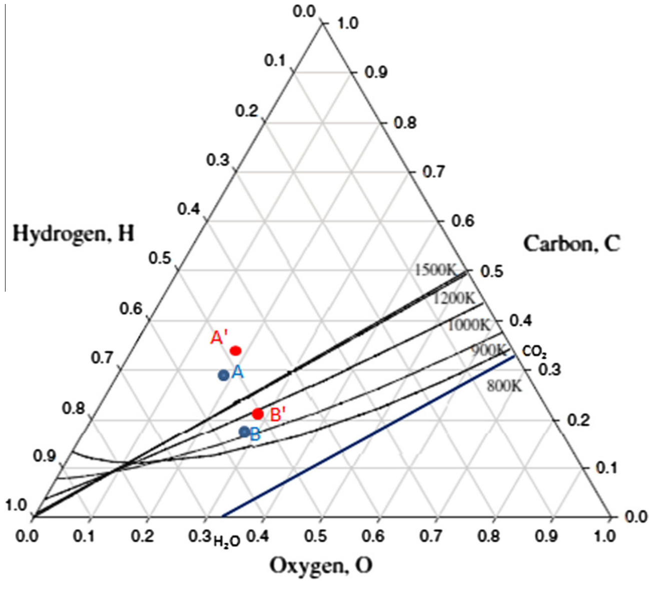

Fig. 13. C–H–O ternary diagram with simulation results from the present study (for one case). Carbon deposition boundary data from literature [59].

point B lies close to the carbon deposition boundaries and this is valid for all 27 cases tested in the present study. The line connecting CO_2 and H_2O represents complete combustion of biomass and in our case point B lies well above this line, thus, indicating a gasification process. If only air is added in the process, the process moves along a line connecting the biomass to the pure oxygen point and the optimum gasification point is where this line intersects the carbon boundary line for a particular temperature. However, with the addition of small amounts of steam, the gasification point moves to point B (or B′) and is slightly below the carbon boundary. This is because the reaction between biomass and steam are endothermic (water gas shift reaction) and those between biomass and air are exothermic (Char partial combustion) [60]. Based on the C–H–O ternary diagram analysis, the present gasification simulation study fits very well with the underlying gasification theory.

4. Conclusions

Biomass gasification was simulated using Aspen Plus with a two-stage gasification model based on Gibbs free energy minimization approach for comparing untreated and torrefied biomass as feedstocks. Model accuracy was improved by including tar, actual experimental decomposition yields and the compositions of the chars produced during pyrolysis in the evaluations. The model outcomes were validated by using a C–H–O Ternary diagram and by comparisons with results from other similar studies. Three process parameters: SBR, GB Temperature and ER were varied. 27 cases were selected with all having carbon in the gaseous form for the final syngas product. It was found that the syngas compositions vary a lot based on the process parameters, and inlet conditions should be selected based on the end requirements for syngas. Here is the summary of results obtained from this study:

1. Out of the three process parameters, ER had the most significant effect on the syngas composition, energy and exergy efficiency.
2. Maximum energy and exergy efficiencies are achieved by operating gasifier at or close to carbon deposition boundary point at that temperature.
3. Torrefied biomass gives higher H_2 and CO contents and higher cold gas energy and exergy efficiencies than untreated biomass.
4. Overall efficiencies of an integrated torrefaction–gasification process depend on the mass yields of the torrefaction process. Torrefaction mass yield of 88% in the present study resulted in better overall energy and exergy efficiencies.
5. Simulation results from this study correlates well with the simulation and experimental results from the Paviet et al. [56] study.

Torrefaction of biomass does seem to have a positive effect on biomass gasification due to improved CO and H_2 contents. This effect is mainly due to the increased carbon content of torrefied biomass due to the devolatilization leading to relatively higher oxygen loss during torrefaction. This is evident from the increased chemical exergy of torrefied biomass as well, and this higher chemical exergy is utilized for improvements in syngas quality. As noted earlier in this study, there is considerable lack of data on the gasification of torrefied biomass and therefore, the authors recommend further studies on additional feedstocks.

Acknowledgements

The authors acknowledge the support of the Bioenergy Innovation Center (CenBio) project team at the Norwegian University of Science and Technology (NTNU) and SINTEF Energy Research for providing financial resources to carry out this study.

References

[1] Sadaka S, Negi S. Improvements of biomass physical and thermochemical characteristics via torrefaction process. Environ Progr Sustain Energy 2009;28:427–34.
[2] van der Stelt MJC, Gerhauser H, Kiel JHA, Ptasinski KJ. Biomass upgrading by torrefaction for the production of biofuels: a review. Biomass Bioenergy 2011;35:3748–62.
[3] Arias B, Pevida C, Fermoso J, Plaza MG, Rubiera F, Pis JJ. Influence of torrefaction on the grindability and reactivity of woody biomass. Fuel Process Technol 2008;89:169–75.
[4] Bridgeman TG, Jones JM, Shield I, Williams PT. Torrefaction of reed canary grass, wheat straw and willow to enhance solid fuel qualities and combustion properties. Fuel 2008;87:844–56.
[5] Bridgeman TG, Jones JM, Williams A, Waldron DJ. An investigation of the grindability of two torrefied energy crops. Fuel 2010;89:3911–8.
[6] Couhert C, Salvador S, Commandré JM. Impact of torrefaction on syngas production from wood. Fuel 2009;88:2286–90.
[7] Deng J, Wang G-J, Kuang J-H, Zhang Y-L, Luo Y-H. Pretreatment of agricultural residues for co-gasification via torrefaction. J Anal Appl Pyrol 2009;86:331–7.
[8] Prins MJ, Ptasinski KJ, Janssen FJJG. Torrefaction of wood. J Anal Appl Pyrol 2006;77:28–34.
[9] Tapasvi D, Khalil R, Skreiberg Ø, Tran K-Q, Grønli M. Torrefaction of Norwegian birch and spruce: an experimental study using macro-TGA. Energy Fuels 2012;26:5232–40.
[10] Tapasvi D, Khalil R, Várhegyi G, Tran K-Q, Grønli M, Skreiberg Ø. Thermal decomposition kinetics of woods with an emphasis on torrefaction. Energy Fuels 2013;27:6134–45.
[11] Tapasvi D, Khalil R, Várhegyi G, Skreiberg Ø, Tran K-Q, Grønli M. Kinetic behavior of torrefied biomass in an oxidative environment. Energy Fuels 2013;27:1050–60.
[12] Tapasvi D, Tran K-Q, Wang L, Skreiberg Ø, Khalil R. Biomass torrefaction – a review. In: INFUB-9 Estoril, Portugal; 2011.
[13] Chen W-H, Kuo P-C. A study on torrefaction of various biomass materials and its impact on lignocellulosic structure simulated by a thermogravimetry. Energy 2010;35:2580–6.
[14] Chen W-H, Kuo P-C. Torrefaction and co-torrefaction characterization of hemicellulose, cellulose and lignin as well as torrefaction of some basic constituents in biomass. Energy 2011;36:803–11.
[15] Jankes G, Trninic M, Stamenic M, Simonovic T, Tanasic N, Labus J. Biomass gasification with CHP production: a review of state of the art technology and near future perspectives. Therm Sci 2012;16:115–30.
[16] Puig-Arnavat M, Bruno JC, Coronas A. Review and analysis of biomass gasification models. Renew Sustain Energy Rev 2010;14:2841–51.
[17] Zhang L, Xu C, Champagne P. Overview of recent advances in thermo-chemical conversion of biomass. Energy Convers Manage 2010;51:969–82.
[18] Balat M, Balat M, Kırtay E, Balat H. Main routes for the thermo-conversion of biomass into fuels and chemicals. Part 2: Gasification systems. Energy Convers Manage 2009;50:3158–68.
[19] Srinivas T, Gupta AVSSKS, Reddy BV. Thermodynamic equilibrium model and exergy analysis of a biomass gasifier. J Energy Res Technol 2009;131.

[20] Schuster G, Löffler G, Weigl K, Hofbauer H. Biomass steam gasification – an extensive parametric modeling study. Bioresour Technol 2001;77:71–9.

[21] Altafini CR, Wander PR, Barreto RM. Prediction of the working parameters of a wood waste gasifier through an equilibrium model. Energy Convers Manage 2003;44:2763–77.

[22] Melgar A, Pérez JF, Laget H, Horillo A. Thermochemical equilibrium modelling of a gasifying process. Energy Convers Manage 2007;48:59–67.

[23] Jarungthammachote S, Dutta A. Thermodynamic equilibrium model and second law analysis of a downdraft waste gasifier. Energy 2007;32:1660–9.

[24] Jarungthammachote S, Dutta A. Equilibrium modeling of gasification: Gibbs free energy minimization approach and its application to spouted bed and spout-fluid bed gasifiers. Energy Convers Manage 2008;49:1345–56.

[25] Yoshida H, Kiyono Fo, Tajima H, Yamasaki A, Ogasawara K, Masuyama T. Two-stage equilibrium model for a coal gasifier to predict the accurate carbon conversion in hydrogen production. Fuel 2008;87:2186–93.

[26] Ghassemi H, Shahsavan-Markadeh R. Effects of various operational parameters on biomass gasification process; a modified equilibrium model. Energy Convers Manage 2014;79:18–24.

[27] Bassyouni M, ul Hasan SW, Abdel-Aziz MH, Abdel-hamid SMS, Naveed S, Hussain A, et al. Date palm waste gasification in downdraft gasifier and simulation using ASPEN HYSYS. Energy Convers Manage 2014;88:693–9.

[28] Ravikiran A, Renganathan T, Pushpavanam S, Voolapalli RK, Cho YS. Generalized analysis of gasifier performance using equilibrium modeling. Ind Eng Chem Res 2012;51:1601–11.

[29] Li X, Grace JR, Watkinson AP, Lim CJ, Ergüdenler A. Equilibrium modeling of gasification: a free energy minimization approach and its application to a circulating fluidized bed coal gasifier. Fuel 2001;80:195–207.

[30] Mansaray KG, Al-Taweel AM, Ghaly AE, Hamdullahpur F, Ugursal VI. Mathematical modeling of a fluidized bed rice husk gasifier: Part I – Model development. Energy Sources 2000;22:83–98.

[31] Paviet F, Chazarenc F, Tazerout M. Thermo chemical equilibrium modelling of a biomass gasifying process using ASPEN PLUS. Int J Chem Reactor Eng 2009;7.

[32] Chen WH, Chen CJ, Hung CI. Taguchi approach for co-gasification optimization of torrefied biomass and coal. Bioresour Technol 2013;144:615–22.

[33] Chen W-H, Chen C-J, Hung C-I, Shen C-H, Hsu H-W. A comparison of gasification phenomena among raw biomass, torrefied biomass and coal in an entrained-flow reactor. Appl Energy 2013;112:421–30.

[34] Kuo P-C, Wu W, Chen W-H. Gasification performances of raw and torrefied biomass in a downdraft fixed bed gasifier using thermodynamic analysis. Fuel 2014;117:1231–41.

[35] Ptasinski KJ, Prins MJ, Pierik A. Exergetic evaluation of biomass gasification. Energy 2007;32:568–74.

[36] Rao MS, Singh SP, Sodha MS, Dubey AK, Shyam M. Stoichiometric, mass, energy and exergy balance analysis of countercurrent fixed-bed gasification of post-consumer residues. Biomass Bioenergy 2004;27:155–71.

[37] Pellegrini L, Deoliveirajr S. Exergy analysis of sugarcane bagasse gasification. Energy 2007;32:314–27.

[38] Abuadala A, Dincer I, Naterer GF. Exergy analysis of hydrogen production from biomass gasification. Int J Hydrogen Energy 2010;35:4981–90.

[39] Hosseini M, Dincer I, Rosen MA. Steam and air fed biomass gasification: comparisons based on energy and exergy. Int J Hydrogen Energy 2012;37:16446–52.

[40] Fryda L, Panopoulos KD, Kakaras E. Integrated CHP with autothermal biomass gasification and SOFC–MGT. Energy Convers Manage 2008;49:281–90.

[41] Karamarkovic R, Karamarkovic V. Energy and exergy analysis of biomass gasification at different temperatures. Energy 2010;35:537–49.

[42] Kempegowda RS, Assabumrungrat S, Laosiripojana N. Thermodynamic analysis for gasification of Thailand rice husk with air, steam, and mixed air/steam for hydrogen-rich gas production. Int J Chem Reactor Eng 2010;8.

[43] Kempegowda RS, Pannir Selvam PV, Skreiberg Ø, Tran K-Q. Process synthesis and economics of combined biomethanol and CHP energy production derived from biomass wastes. J Chem Technol Biotechnol 2012;87:897–902.

[44] Nikoo MB, Mahinpey N. Simulation of biomass gasification in fluidized bed reactor using aspen plus. Biomass Bioenergy 2008;32:1245–54.

[45] Wannapeera J, Fungtammasan B, Worasuwannarak N. Effects of temperature and holding time during torrefaction on the pyrolysis behaviors of woody biomass. J Anal Appl Pyrol 2011;92:99–105.

[46] Ptasinski KJ. Thermodynamic efficiency of biomass gasification and biofuels conversion. Biofuels, Bioprod Biorefin 2008;2:239–53.

[47] Aigner I, Wolfesberger U, Hofbauer H. Tar content and composition in producer gas of fluidized bed gasification and low temperature pyrolysis of straw and wood – influence of temperature; 2009.

[48] Fjellerup J, Ahrenfeldt J, Henriksen U, Gøbel B. Formation, decomposition and cracking of biomass tars in gasification. Denmark: Technical University of Denmark; 2005. p. 1–60.

[49] Chang SK, Sung PM. Characterization of pyrolysis tar derived from lignocellulosic biomass. J Ind Eng Chem 2006;12:853–61.

[50] Panopoulos KD, Fryda L, Karl J, Poulou S, Kakaras E. High temperature solid oxide fuel cell integrated with novel allothermal biomass gasification. J Power Sources 2006;159:586–94.

[51] Kotas TJ. The exergy method of thermal plant analysis. Krieger Publishing Company; 1995.

[52] Szargut VJ, Styrylska T. Angenaherte bestimmung der exergie von brennstoffen. Brennstoff-Warne-Kraft 1964;16:S.589.

[53] Morris DR, Szargut J. Standard chemical exergy of some elements and compounds on the planet earth. Energy 1986;11:733–55.

[54] Wikipedia.org. Heat of combustion. http://en.wikipedia.org/wiki/Heat_of_combustion

[55] Hacker V, Kordesch K. Handbook of fuel cells – fundamentals, technology and applications. In: Ammonia crackers. Chichester: John Wiley & Sons, Ltd.; 2003 [chapter 10].

[56] Paviet F, Chazarenc F, Tazerout M. Thermo chemical equilibrium modelling of a biomass gasifying process using aspen plus. Int J Chem Reactor Eng 2009;7.

[57] Doherty W, Reynolds A, Kennedy D. The effect of air preheating in a biomass CFB gasifier using aspen plus simulation. Biomass Bioenergy 2009;33:1158–67.

[58] Prins MJ, Ptasinski KJ, Janssen FJJG. Torrefaction of wood. J Anal Appl Pyrol 2006;77:35–40.

[59] Tay DHS, Ng DKS, Kheireddine H, El-Halwagi MM. Synthesis of an integrated biorefinery via the C–H–O ternary diagram. Clean Technol Environ Policy 2011;13:567–79.

[60] Prins MJ, Ptasinski KJ, Janssen FJJG. Thermodynamics of gas–char reactions: first and second law analysis. Chem Eng Sci 2003;58:1003–11.